Abstract

The Hausdorff chirality measure quantifies the chirality of a geometric representation of an object by measuring the degree of coincidence of the object with its mirror image. It can also allow comparison between a chiral dopant and host molecules which may illuminate mechanisms for chirality transfer. It has been applied to real molecules very infrequently in comparison to application of chiral indices as it is complex and time consuming to calculate. In this paper we introduce and verify a simulated annealing algorithm for the Hausdorff chirality measure that has proven rapid, robust and relatively simple to apply. We verify the method, finding good agreement between its results and those of Mislow and co-workers. We introduce a Hausdorff structure measure that does not permit overlap and allows a structure to be built one molecule at a time. We present results for a simple model and real biphenyl molecules and discuss promising building blocks of crystal and incommensurate structures formed in relation to experimental results.

The Hausdorff chirality measure and a proposed Hausdorff structure measure

Emmanuel O Yewande [*], Maureen P. Neal [*†], and Robert Low [‡]

November 11, 2008

1 INTRODUCTION

The need to move from Lord Kelvin's definition of chirality in 1904,[1] applied to chiral molecules, as having no mirror symmetry, to quantitative measures of molecular chirality has wide scientific motivation especially in chemistry, biology and biochemistry. Equally the mechanisms behind the induction of a chiral mesophase by the addition of a chiral dopant to an achiral liquid crystalline host phase remain unclear and are also a motivation for this work. In particular the similarity of the molecular shape between the dopant and the host has been proposed as a possible mechanism. The range of chirality measures and indices available to tackle this problem reflect different aspects of the chirality of molecules and the mechanisms for chirality transfer.

According to Lord Kelvin a geometrical figure is chiral if its mirror image can not be brought to coincide with it. Some chirality measures, χ, such as the Hausdorff measure discussed here[2,3] have been defined to measure the chirality of an object without regard to its absolute configuration hence the measure of the object and its mirror image are the same, and χ only vanishes for achiral objects. They are even in the sense that if O is a shape and O' is its mirror image, then $\chi(O) = \chi(O')$. Other indices, such as the scaled chiral index G_{0S},[4,5,6,7,8,9] based on the Osipov chirality index G_0,[10] and the chirality order parameter $\mathcal{Q}$ of Nordio and co-workers[11,12,13] are particularly designed to quantify the relationship between the chirality of molecules and measurable pseudoscalar properties such as helical twisting power (HTP).

Such indices have the property that they are odd in the sense that $\chi(O) = -\chi(O')$. Such indices are necessarily zero when the shape S is achiral, but will also exhibit chiral zeros (i. e. $\chi(O) = 0$ for some objects not congruent to their mirror images) in $3D$. This is due to the continuity and chiral connectedness

[*]Department of Computing & Mathematics, Manchester Metropolitan University, Manchester M1 5GD, United Kingdom. Electronic mail: e.yewande@mmu.ac.uk, m.neal@mmu.ac.uk

[†]Corresponding author, from October 2008 maureen.neal@plymouth.ac.uk

[‡]Department of Mathematical Sciences, Coventry University, Coventry CV1 5FB, United Kingdom. Electronic mail: mtx014@coventry.ac.uk

that exists in three and higher dimensions, in which it is possible to interconvert two enantiomorphs of the same chiral object by a continuous deformation along a pathway that consists entirely of chiral configurations.[14,15] Both these latter indices are widely applied as measures of the degree of chirality. Both allow for a rapid calculation of the degree of chirality of molecules, irrespective of molecule size, and both show a good correlation with the helical twisting power of certain liquid crystal dopants in a nematic liquid crystal solvent.[8,6,16,9,11,12,13]

The chirality order parameter $\mathcal{Q}$ of Nordio and co-workers includes the dopant-host interaction whereas the scaled chiral index G_{0S} is dependent on the dopant molecules alone. The correlations of both G_{0S} and $\mathcal{Q}$ with experimental helical twisting power show similar trends and comparison of them has not illuminated mechanisms of host-dopant interaction.[9] The scaled chiral index has recently been employed effectively to predict chirality of proteins[17] utilising a cut-off,[17,18] opening up a new area of applications.

A chirality measure was proposed by Mislow and co-workers (BHM) as a direct consequence of Lord Kelvin's definition of chirality. This chirality measure employs the Hausdorff distance between sets as a way of calculating the extent to which two optimally superimposed objects or sets fail to be congruent, and its normalization by the diameter of the object gives the degree of chirality χ_H of the object.[2,3] Thus χ_H must be equal to zero if an object can be brought into total coincidence with its mirror image, and greater than zero but less than one otherwise.

An application[19] of this measure to study the mechanism of chirality transfer is encouraging and will be briefly mentioned below. However, achieving the optimal superimposition required to calculate χ_H is not an easy task and different methods have been employed by different groups.

BHM applied the Hausdorff chirality measure extensively to the problem of the most chiral simplex in two- and three-dimensional Euclidean space.[2,3] For the low-dimensional problems such as the search for most chiral triangle, and tetrahedra with D_2 and C_2 symmetries, they employed a grid search method. The search space was discretized and the shape was changed in incremental steps along the dimensions until a relatively flat maximum was found in the region of high χ_H. They then used the Broyden-Fletcher-Goldfarb-Shanno (BFGS) maximization procedure to locate the point in the region with the largest value of χ_H. In contrast with the higher dimensional problem such as the search for the most chiral tetrahedron with C_1 symmetry, they explored the shape space initially by performing random Monte Carlo tests for regions characterized by a high degree of chirality. After this they used the BFGS procedure to locate the point, in one of the two regions found, that represents the most chiral tetrahedron.

In this paper, we introduce our method of search for the global minimum of χ_H using a simulated annealing (SA) algorithm that is relatively simple to apply and general in its nature. We verify it by applying it to the problem of searching for the most chiral simplex in two- and three-dimensional Euclidean space,[2,3] following the steps of Mislow and co-workers especially as regards the shape space of triangles and tetrahedra.

The Hausdorff chirality formalism has been applied to real molecules[19] using a branch and bound procedure to obtain the configuration at optimal superimposition required to calculate the minimum Hausdorff distances. The investigators studied the role of molecular similarity in the transfer of chirality from a chiral guest to an achiral host. They obtained the result that for some of the molecules investigated, those containing hydrocarbon substituents, the helical twisting power (HTP) decreases with increasing chirality of the dopant. This was further investigated[16] and a Langmuir form of the Hausdorff measure was found to show a good correlation with experimental helical twisting power, leading to the conjecture that χ_H is optimised when the non-chiral intersection is a maximum and that the host - dopant interaction mechanism is determined by the non-intersection chiral region of each molecule.

The Hausdorff measure calculates the way in which two optimally superimposed molecules fail to be congruent; however such superposition of molecules is non-physical. We apply this to a simple model biphenyl molecule and to minimized structures of a real biphenyl molecule obtained from computer aided chemistry (CaChe) experiments.[22] In this paper we propose a Hausdorff structure measure that additionally includes the constraint of no overlap of atoms in different molecules from within a minimum of a Van der Waals radius up to a unit cell dimension for a crystal. Note that while the minimal Hausdorff distance between a molecule and its mirror image (without any exclusion constraint) is a good mathematical measure of how chiral it is, a different problem is how closely together two physical molecules can pack, and this is what is addressed by the new structure measure with the exclusion constraints included.

We present an appplication of the Hausdorff structure factor to biphenyl in which we build a structure using the algorithm to repeatedly add single molecules, up to a set of three, and make comparison with experimental results for crystal and incommensurate phases. We will show that we have robust and relatively rapid algorithms that can be applied to the real molecules effectively.

The long term aim is to investigate if a suitable combination of the Hausdorff chirality measure, structure measure and chirality indices will correlate well with experimentally observed HTP[19, 16] and allow study of host-dopant mixtures where the induced helical twisting power is dependent on the host.[20, 21]

The rest of this paper is organized as follows: in the next section we present our method and specific details of its application. A review of Mislow and coworkers's definition of the shape spaces of triangles and tetrahedra is presented in this section (sections 2.2.1 and 2.2.2, respectively) to make this article more self-contained. In section 3, we present our results as well as their comparison to those in the literature and finally we present our conclusions.

2 Method

2.1 Hausdorff chirality measure

The Hausdorff distance $d_H(O,Q)$ between two non-empty and bounded sets (e.g. of point masses) O and Q is defined as

$$d_H(O,Q) \equiv \max\{\sup_{o\in O} d(o,Q), \sup_{q\in Q} d(q,O)\}, \tag{1}$$

where $d(o,Q)$ is $\inf_{q\in Q} d(o,q)$. Then if $d_{H_{\min}}(O,Q)$ is defined to be the minimum Hausdorff distance between O and Q over all positions and orientations of O and Q, we define the degree of chirality of a set O to be

$$\chi_H(O) = \frac{d_{H_{\min}}(O,O')}{d(O)}, \tag{2}$$

where O' is the mirror image of O and $d(O)$ is the diameter of O, which acts as a normalization constant, thus ensuring scale invariance χ_H.

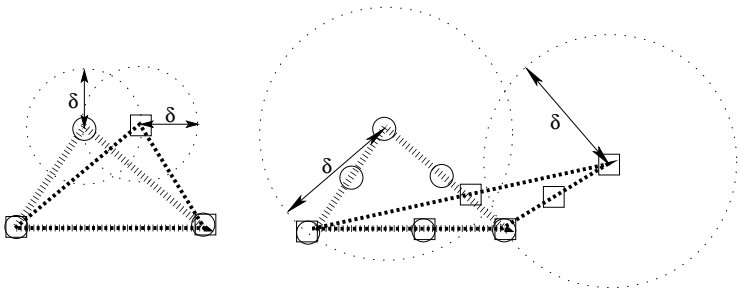

Figure 1: An illustration of the Hausdorff formulation[23] $d_H(O,Q)$ (O and Q are the triangles shown) is the smallest number δ such that each spherical ball (dot circles) of radius δ centered at any point (vertex) of O contains at least one point of Q, and vice-versa.

We calculate the Hausdorff distance between two sets O and Q as follows (see the illustration in Fig. 1).

For each point $i \in O$, we find the minimum distance $R_i = R_{ij}^{\min}$ between i and each point $j \in Q$. For all the points $i \in O$ considered, we find $d_{H_{OQ}} = \max\{R_i\}$; then we swap the sets, and repeat the procedure to obtain $d_{H_{QO}}$, so that $d_H(O,Q) = \max\{d_{H_{OQ}}, d_{H_{QO}}\}$. We then take the minimum value of $d_{H_{OQ}}$ as the position and orientation of Q is allowed to vary. The algorithm we shall introduce in section 2.3 enables a gradual approach to the state of $d_{H_{\min}}$.

The Hausdorff chirality measure is an optimization problem whose accuracy depends on the attainment of a state of optimal overlap of two objects, e. g. two enantiomorphs, as illustrated in Fig. 1. In real molecules, however, the atoms cannot overlap and this defines a constraint of an excluded radius, corresponding

to the Van der Waals distance, r_{VdW} by which atoms in distinct molecules must at least be separated. In addition in a unit cell in a crystal they are separated by the unit cell dimensions. We propose a Hausdorff structure factor, $\chi_{HS}(O,Q)$ which adds this separation constraint so $d_{HS_{\min}}(O,Q)$ is the minimum Hausdorff distance $d_{HS_{\min}}(O,Q)$ between O and Q over all positions and orientations of O and Q, satisfying the constraint. For real molecules in any state of matter $d_{HS_{\min}}(O,Q)$ is greater than or equal to r_{VdW}. We also consider the case where $d_{HS_{\min}}(O,Q)$ is the minimum unit cell dimension for a biphenyl crystal in an application presented here. Fig. 2 illustrates the χ_{HS} formulation.

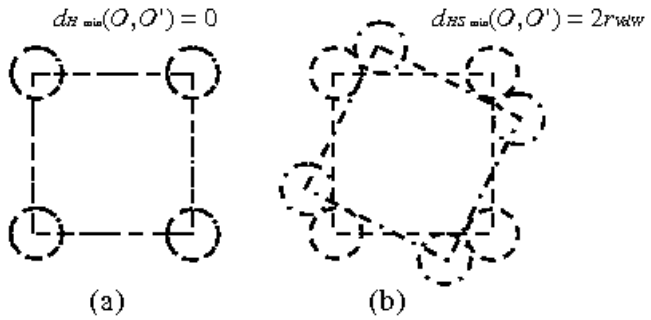

Figure 2: Illustration of the effect of the χ_{HS} formulation on an object composed of constituents located at the vertices of a square. $d_{H_{\min}}(O,O')$ is zero in this case [(a)] since the object is achiral, whereas $d_{HS_{\min}}(O,O')$ is non-zero [(b)] due to the constraint of an excluded radius r_{VdW} which is the closest distance any two points o, o' can get to each other.

2.2 Search Space

In this section, we discuss the configuration space for our simulated annealing algorithm. As pertains to our application of the method to the most chiral simplex in two- and three-dimensions, the search space is the shape space of triangles and tetrahedra, respectively, as defined by Mislow and co-workers.[2,3] Hence, for clarity in our discussion of how we sample these spaces, we shall review the pertinent details of their work on these shape spaces in sections 2.2.1 and 2.2.2; in relation to how we implement them in our work.

2.2.1 Review of Shape Space of Triangles

Following Mislow and co-workers,[2] we illustrate in Fig. 3 the region of shape space for triangles, within which we search for the most chiral one. One-half of

the area formed from an intersection of two circles of unit radii in this figure contains the unique shapes of all chiral (scalene) and achiral (isosceles and equilateral) triangles.[2] The base of all triangles is centered at origin (0, 0), and fixed

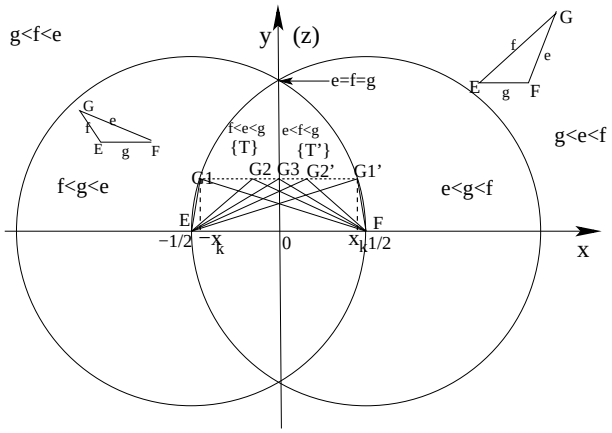

Figure 3: Region of shape space for triangles (upper half of the intersection of the two circles). T denotes the region that contains the set of triangles for which $f \leq e < g$, and T' denotes the region of the corresponding set of enantiomorphs (for which $e \leq f < g$). E.g. the triangles with apex at positions G1', and G2' are the enantiomorphs of the triangle with apex at position G1, and G2, respectively. Note: the dashed horizontal line defines the apex of different triangles having the same altitude y. This figure (with $y \to z$) also illustrate a projection of the intersection of the two unit hemispheres, that define the shape space of tetrahedra, onto the xz plane. In this case G1G1' is a projection of the plateau that contains vertices G and H. x_k is the upper bound on x for any point on the plateau.

between the points (-1/2, 0) and (1/2, 0); the apex is at (x, y), $-1/2 \leq x \leq 1/2$, $0 \leq y \leq \sqrt{3}/2$.

We choose a random point (x, y), corresponding to the vertex G of a randomly chosen triangle EFG, within one-half of the shape space of triangles (Fig. 3), where, for general triangles, $0.01 \leq y \leq \sqrt{3}/2$, $0 \leq x \leq (\sqrt{1-y^2} - 1/2)$ and, for right triangles, $0 \leq x \leq 1/2$ and $y = \sqrt{1/4 - x^2}$.

2.2.2 Review of Shape Space of Tetrahedra

According to Mislow and co-workers[2, 3] a 3D analog of the above gives the shape space of tetrahedra $S(T)$, i. e., the intersection of two unit hemispheres centered on (-1/2, 0, 0) and (1/2, 0, 0) contains both enantiomorphs of all tetrahedra with each tetrahedron oriented in such a way that if two vertices (say E and F) are placed on the xy plane, the other two vertices (say G and H) are located in

another plane parallel to, and at a distance d_p from, the xy plane.

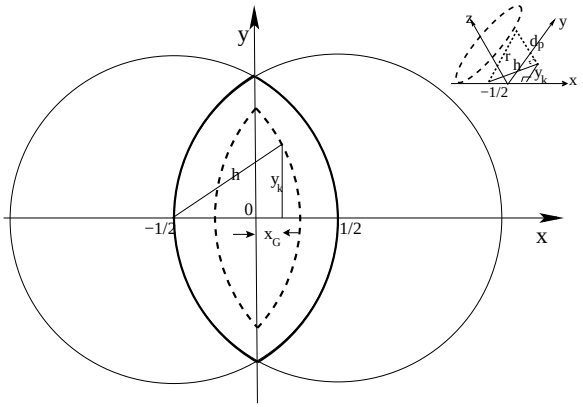

Figure 4: Projection (area enclosed by bold arches) of the region of shape space for tetrahedra onto the xy plane. The bold dashed arches represent the projection of an arbitrary plateau that contains the vertices G and H of an arbitrary tetrahedron. r (= 1) is the radius of an hemisphere, and h ($< r$) is the projection of r onto the xy plane (see the inset). d_p is the distance of the plateau from the xy plane. In the inset, the plateau is represented by the dashed ellipsoid.

Similarity invariance of all tetrahedra is achieved by the transformation $l_T \rightarrow l_T/d_T$ on each side of a tetrahedron so that no side is greater than unity. l_T is the length of a side of the tetrahedron, and d_T the length of its longest side. Since vertices E and F are fixed, the tetrahedral shapes will be unique (i. e., there will be no isometric faces that can be obtained by mirror reflection) if vertices G and H are in the same quadrant or adjacent quadrants (see Fig. 4) of the hemispherical intersection only once. This can be achieved, as shown by Mislow and co-workers,[2,3] by restricting vertex G to the first quadrant, and allowing vertex H to be in any of the four quadrants.

Hence, the shape space $S(T)$ is unique and similarity invariant if we choose the vertices E = (-1/2, 0, 0), F = (1/2, 0, 0), $G = (x_G,\ y_G,\ d_p)$, $H = (x_H,\ y_H,\ d_p)$; where d_p is the distance from the plane of vertices E and F, to the plane of G and H; and thus defines a plateau, bounded by the hemispherical intersection. A projection of this plateau onto the xy-plane is illustrated in Fig. 3 by the line G1G1', so that d_p is the perpendicular distance of line G1G1' to the x-axis. From Fig. 3 an upper bound $d_{p_k} = \sqrt{3}/2$ on d_p occurs at the intersection for which $e = f = g$, hence $0 < d_p < \sqrt{3}/2$.

This plateau sets bounds $x_k(d_p)$ on the values of x_G and x_H, and bounds $y_k(d_p, x)$ ($x = x_G$ or x_H) on the values of y_G and y_H; thus $x_k(d_p)$ and $y_k(d_p, x)$ define the boundary of the hemispherical intersection (shape space of tetrahedra). Since G is restricted to the first quadrant of the plateau, we choose x_G

and y_G randomly in the range: $0 \leq x_G \leq x_k$, and $0 \leq y_G \leq y_k(d_p, x_G)$; where $x_k = \sqrt{1-d_p^2} - 1/2$ (see Fig. 3), and $y_k(d_p, x) = \sqrt{(1-d_p^2) - (1/2 + |x|)^2}$ (see Fig. 4) .

On the other hand, H can be anywhere on the plateau as long as $|GH| \leq |EF|$, hence we choose x_H and y_H randomly in the range: $-x_k \leq x_H \leq x_k$, and $-y_k \leq y_H \leq y_k(d_p, x_H)$. If the values we choose for x_H and y_H satisfy: $(x_H - x_G)^2 + (y_H - y_G)^2 \leq 1$ (i. e. since $|GH| \leq 1$), we accept the choice of x_H and y_H, else we reject the choice.

The general case has no symmetry other than the trivial case of being invariant under a rotation by 360°, i. e. C_1 symmetry hence the only constraint is that the edge-length must not be greater than unity. We have also addressed the following tetrahedral symmetries by imposing additional constraints.

C_2 Symmetry: This imposes the additional constraint of a 2-fold rotation axis that is perpendicular to the xy-plane and passes through the origin of the coordinate system, and requires four distinct edge-lengths[15] $|EF|$, $|GH|$, $|EH|$ $(= |GF|)$, $|EG|$ $(= |FH|)$. We achieve this by allowing vertex G to roam the first quadrant of the plateau as earlier, restricted by the circle of unit diameter exclusively (so that $|GH| < 1$). Hence, we require that $x_G^2 + y_G^2 < 0.5^2$, $x_H = -x_G$ and $y_H = -y_G$.

D_2 Symmetry: A tetrahedron with D_2 symmetry, in addition to the two-fold rotation axes, has three distinct edge-lengths $|EF|$ $(= |GH|)$, $|EG|$ $(= |FH|)$, and $|EH|$ $(= |GF|)$. This is achieved by letting vertices G and H lie on a circle of radius $1/2$ centered on $(0, 0, d_p)$. In this case we reduce the search space by setting: $y_G = \sqrt{1/4 - x_G^2}$, $x_H = -x_G$ and $y_H = -y_G$. Note that for this symmetry, vertex $G(x_G,\ y_G)$ falls within the plateau only if $0 \leq x_G \leq x_{G_k}$; where x_{G_k} is the upper bound on (D_2 symmetric) y_G for which $y_G(x_{G_k}) = y_k(d_p, x_{G_k})$; i. e. $x_{G_k} = 1/2 - d_p^2$, $x_{G_k} < x_k$.

The achiral geometries with C_{2v} and D_{2d} symmetry should always give $\chi_H = 0$. Hence we test the algorithm, as well as the constrained reduction of the search space so far employed, by reducing the configuration space in a similar way to allow only pathways that conform to C_{2v} and D_{2d} symmetry as follows.

C_{2v} Symmetry: In addition to the two-fold rotation axis, this has the three distinct edge-lengths $|EF|$, $|GH|$, and $|EG|$ $(= |FG| = |EH| = |FH|)$. To achieve this, we set $x_H = x_G = 0$, $y_H = -y_G$, for $0 \leq y_G < 0.5$ (i. e. we consider any random d_p but set 0.5 as the (exclusive) upper bound on y_G instead of y_k).

D_{2d} Symmetry: In addition to the two-fold rotation axis, this can only have two distinct edge-lengths $|EF|$ $(= |GH| = 1)$, and $|EG|$ $(=|FG| = |EH| = |FH|)$. To achieve this, we set $x_H = x_G = 0$, $y_H = y_G - 1$, for $0.5 \leq y_G \leq y_k$ (i. e. only consider random d_p such that $0 < d_p < 1/\sqrt{2}$ so that $y_k(d_p, 0) > 1/2$).

As expected $\chi_H = 0$, always, along these pathways.

2.2.3 Biphenyl Molecules

Model 1

The simplest model of a biphenyl molecule is the set of points $\mathcal{S}_B$ defined as

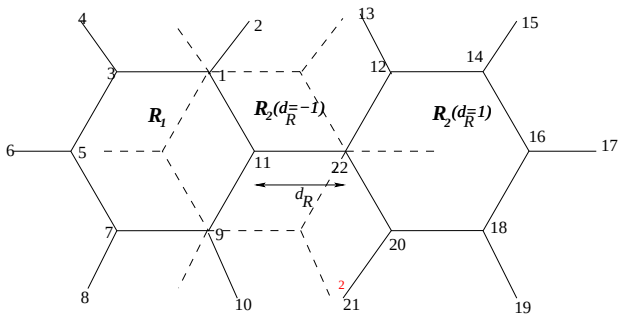

Figure 5: An illustration of our biphenyl model (the lines joining the atoms are to guide the eyes). The atoms are numbered as in Eqs. 3 and 4. The dashed phenyl ring $\mathcal{R}_2(d_R = -1)$ combined with $\mathcal{R}_1$ represents the particular case of a biphenyl model for which $d_R = -1$, and is allowed here in order to investigate the possible range of χ_H on our simple model.

follows (see Fig. 5). Let $\mathcal{R}_1$, the first phenyl ring, be the set of points

$$\mathcal{R}_1 = \{\mathbf{C}_i^a, \mathbf{H}_j : 1 \leq i \leq 6; 1 \leq j \leq 5; i, j \in \mathcal{N}\} \tag{3}$$

where $\mathbf{C}_i^a = d_{C-C}(\cos(i\pi/3), \sin(i\pi/3), 0)$, and $\mathbf{H}_j = (1+\delta h)\mathbf{C}_j^a$ are the coordinates of the ith Carbon atom, and jth Hydrogen atom ($\delta h = 0.9$), respectively. d_{C-C} is the C-C length, δh is the C-H length. The ring is centered on the origin of the Cartesian coordinate system. Then the second phenyl ring, $\mathcal{R}_2$ is obtained from the first via a transformation $T(d_R)R_\pi$, i. e.

$$\mathcal{R}_2 = T(d_R)R_\pi\mathcal{R}_1, \tag{4}$$

where $d_R = |\mathbf{C}_{12}^a - \mathbf{C}_6^a|$ is the distance between the two phenyl rings. R_π is a flip (i. e. a 180° rotation) about the y-axis, and $T(d_R)$ is a translation by $0.1(2d_{C-C} + d_R)$ nm along the positive x direction. Thus

$$\mathcal{S}_B = \mathcal{R}_1 \cup \mathcal{R}_2. \tag{5}$$

Hence, our configuration space for the model biphenyl comprises all possible combinations in Eq. 5 of $\mathcal{R}_2 \rightarrow R_\theta\mathcal{R}_2$ (i. e. $\mathcal{S}_B \rightarrow \mathcal{S}_{B_\theta} = \mathcal{S}_B(\theta)$), where R_θ is a rotation by θ radians about the x-axis. For uniqueness of conformation we require that $0 \leq \theta \leq \pi/4$ in an analogous way to the one discussed above (in section 2.2.2). That is, our search space in this case may be represented by the set

$$\mathcal{U} = \{\mathcal{S}_{B_\theta} : 0 \leq \theta \leq \pi/4\}. \tag{6}$$

Since all conformations for which $\theta > \pi/4$ are congruent to some conformation within the unique configuration space defined by $0 \leq \theta \leq \pi/4$, and would

not yield any χ_H different from the ones to be encountered within the unique configuration space (see Fig. 6).

Model 2

Biphenyl in its crystal phase, phase I, is close to planar.[28,29] It is found to have two further incommensurate phases,[31] phases II and III, where molecular twisting is present between the two planes of the phenyl rings in the range 34° to 45°.[29,30] In model 2 we utilise X-ray diffraction measurements of crystalline biphenyl[33] where the approximate C-H separation (δh), C-C length (d_{C-C}), and the ring-ring separation (d_R) are 0.1, 0.137, and 0.149 nm, respectively. It is this model we utilise with the Hausdorff structure measure to build simple structures with twist angles of 0° and 34°, and compare them with experimental data.

2.3 Simulation

We search for the global minimum χ_H using the simulated annealing (SA) method. Since we are also interested in finding the most chiral triangle, tetrahedron, and biphenyl conformation, corresponding to the one with the highest χ_H ($\chi_H^{\max}$), we then have another typical problem of a search for a global maximum, which we again address using the SA algorithm. Noting that we are mainly interested in this method as pertains to real molecules, we use it to get very close to the global minimum of $\chi_H(M)$ for a molecule M from a random starting configuration. Here, we verify our method by combing the search space for the geometric shape with the highest χ_H with a view to extracting the same or similar shape to that found to be the most chiral by Mislow and co-workers.[2,3]

We define the object O as a set of point masses in a Cartesian coordinate system with the mirror image $O' = -O$.[24] To obtain $\chi_H(O, O')$ we use a SA algorithm to search for the optimal superimposition of O and O' by performing a simulation of a random series of rotations and translations of O, keeping O' stationary. We start the simulation with a random orientation and translation of O, and then centre both enantiomorphs on the origin. We iterate down over the "temperature", keeping it fixed and perfoming N_{MC} Monte Carlo (MC) steps on each iteration; but re-scaling the temperature by a factor $T_S < 1$, for the next iteration. We choose $N_{\mathrm{MC}} = 500\ N$, where N is the number of atoms in O; and $T_S = 0.75$ based on a series of initial test runs to determine the best parameter combinations in terms of speed and accuracy.

In a MC step, we change the state i.e. the orientation and position of O relative to O' by rotating and translating it, after which we calculate the new χ_H and accept or reject the move using the Metropolis algorithm. Both the rotation and translation giving the superimposition process are weighted by, and hence reduce with, the temperature as the superimposition process "cools". The acceptance probability in the Metropolis algorithm is also "annealed" via the decreasing temperature. Note that Mislow and co-workers used a different approach to obtain χ_H in which the Hausdorff distance $h(O, O')$ depends on six variables; three of which describe translations of O' in E^3 and the other three rotations of the same object in E^3. They used the BFGS procedure to minimize

$h(O, O')$ as a function of its six variables.

Next, we determine the object O in the shape space with the highest $\chi_H(O, O')$, dependent on the symmetry, by again using a SA algorithm. We perform N_{MC} MC steps in each iteration over the temperature during which we consider many configurational changes, calculate $\chi_H(O, O')$ for each new shape, and consider accepting the moves to states of higher $\chi_H(O, O')$ according to a Metropolis algorithm whose acceptance probability decreases with the temperature. The determination of the extremum of $\chi_H(O, O')$ is a difficult problem with many close maxima giving false results, hence, we make repeated checks on the better states found before accepting the move. If the better state is found to be genuine after an initial check, we retain it as current $\chi_c = \chi_H$ and continue with the search (i.e configurational changes).

In the meantime, we continue to check this current state of highest chirality at regular intervals until a total of $N_{ch} = 5$ checks have been performed after which if no better state is found we set it as the best (current most chiral) state, setting (best χ_H) $\chi_B = \chi_c$. Making a record of the best chiral state during the search is also very useful in zooming down to the extremal shape (i. e. the most chiral) in an analogous way to weighting down the superimposition process with temperature as described above. Due to the high dimensionality of the shape space for C_1 symmetry, Mislow and co-workers could not immediately use the BFGS procedure to localize the point that represents the most chiral tetrahedron; they had to first make random tests for regions of high chirality.[2,3] Here, we first allow the simulation to run unhindered until sufficient "cooling" has taken place, during which it is expected to have traversed some region of higher chirality. We then constrain the search by considering only a relatively small region of radius δ_w centered on the vertices G and H of the best shape found so far. That is, we restrict the ith ($i = x$ or y or z) component, i_G of vertex G to $[i_{G_B}$ (or $i_{H_B}) - \delta_w] \leq i_G$ (or $i_H) \leq [i_{G_B}$ (or $i_{H_B}) + \delta_w]$, where i_{G_B} is the ith component of the best G (corresponding to χ_B) and the vertices (G and H) so chosen are still subject to the constraints discussed in section 2.2.2. We re-scale δ_w by the temperature on each iteration over the temperature. When the best shape changes to some new state of higher chirality, the search within the radius δ_w continues around the newly found best state, and so on.

3 Results

Before allowing our algorithm to search the shape space itself for the most chiral shapes, starting from a random initial configuration, we tested its search for $\chi_H^{\min}$ using all the BHM most chiral configurations as input parameters in turn. We found exactly the same $\chi_H^{\min}$ as reported by BHM to 3 dp in all cases except for C_1 symmetric tetrahedron for which we were able to obtain a better superimposition with lower value $\chi_H^{\min} = 0.248$.

Table 1: A summary of our results of the most chiral right and general triangle, and their comparison to the BHM results. BHM denotes the results of Mislow and co-workers,[2,16] and YNL denotes our results. Vertex E = (-0.5, 0) and vertex F = (0.5, 0).

Shape	Method	Internal Angles	χ_H	Rel. χ_H [1]
right triangle	BHM	(54.8, 90.0, 35.2)	0.141 [2]	1
	YNL	(54.8, 90.0, 35.2)	0.14	1
triangle (scalene)	BHM	(44.2, 114.3, 21.5)	0.196	1
	YNL	(43.7, 115.3, 21.0)	0.198	1

Table 2: A summary of our results for tetrahedra, and their comparison to the BHM results. BHM denotes the results of Mislow and co-workers,[2,3] and YNL denotes our results. Vertex E = (-0.5, 0, 0) and vertex F = (0.5, 0, 0).

Symmetry	Method	Internal Angles	χ_H	Rel. χ_H [3]
D_2	BHM	(35.1, 60.5, 35.1, 84.4)	0.221	1
	YNL	(35.01, 60.51, 35.01, 84.44)	0.221	1
C_2	BHM	(45.6, 58.5, 38.0, 34.7)	0.252	1
	YNL	(45.23, 58.62, 37.92, 35.24)	0.253	1.004
C_1	BHM	(44.4, 59.7, 37.7, 36.0)	0.248[4]	1
	YNL	(45.15, 58.55, 37.74, 35.12)	0.253	1.02

3.1 Comparison with BHM results

We found the three optimized orientations of both triangular enantiomorphs as reported by Mislow and co-workers[2] but we have only shown the result for the one with the lowest $\chi_H^{\min}$ in Table 1.

In Table 1 we compare our triangle results to the BHM results. In excellent agreement,[2] we found the most chiral right-triangle to be the one with internal angles $F\hat{E}G = 54.8°$, $G\hat{F}E = 35.2°$, and for which $\chi_H = 0.14$. For the most chiral scalene triangle we found a slightly improved result with the corresponding internal angles 43.7, 115.3, 21.0, respectively, and $\chi_H = 0.198$.

A comparison of our tetrahedron results to the corresponding BHM results (Refs.[2,3]) is shown in Table 2. The internal angles of the tetrahedra are given as θ_{EGH}, θ_{GFE}, θ_{GEF}, and θ_{GEH}, respectively; where θ_{EGH} is the angle between the edges EG and GH. We calculate the internal angle θ_{EGH} from the position vectors **E**, **G**, and **H**, as

$$\theta_{EGH} = \cos^{-1}\left(\frac{\vec{GE}\cdot\vec{GH}}{|\vec{GE}||\vec{GH}|}\right) = \cos^{-1}\left[\frac{(\vec{E}-\vec{G})\cdot(\vec{H}-\vec{G})}{|\vec{E}-\vec{G}||\vec{H}-\vec{G}|}\right]. \tag{7}$$

As shown in Table 2, we obtain almost identical results. Our method yielded slightly better results than that of BHM for the most chiral C_2 and C_1 tetrahedron.

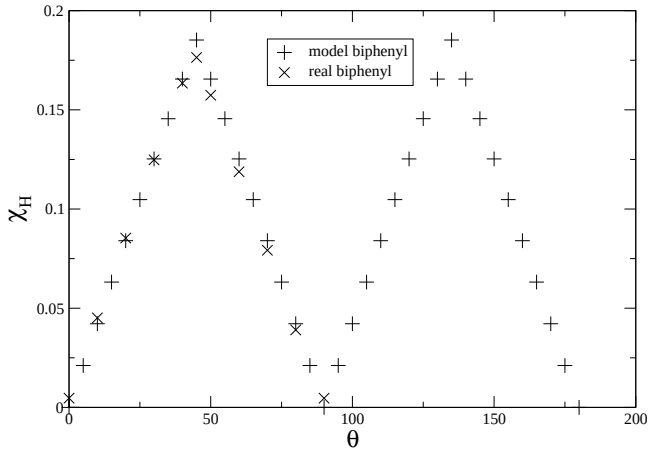

Figure 6: The Hausdorff degree of chirality χ_H of our biphenyl model as a function of the dihedral angle θ between the two phenyl rings, for dihedral angular rotations $0 \leq \theta \leq \pi$ (here $d_R = 1$). The result for a real biphenyl molecule is also shown.

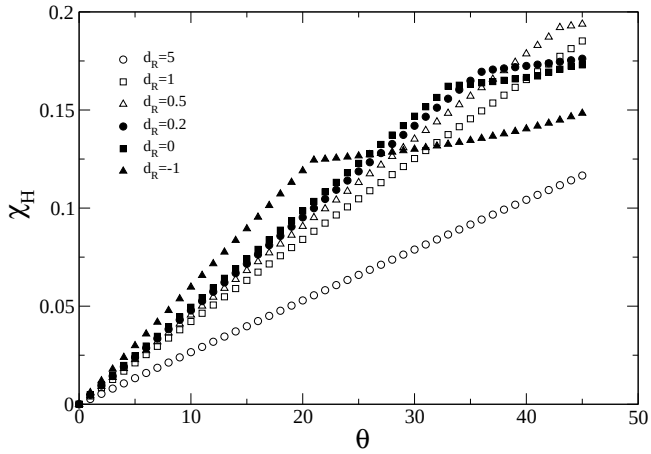

Figure 7: The Hausdorff degree of chirality χ_H of our biphenyl model as a function of the dihedral angle θ for different separation d_R between the two phenyl rings. $d_R = -1$, 0, 0.2, 0.5, 1 and 5. Bold closed symbols represent data for which $d_R < 0.5$ and open symbols denote data with $d_R \geq 0.5$. Here, we consider only stepwise conformational changes within the unique configuration space defined by θ in the range $0 \leq \theta \leq \pi/4$.

3.2 Biphenyl Model results

Having shown the algorithm is robust and finding it to be rapid we then present our results of a test of the method on our biphenyl model in Figs. 6 and 7. In this case we consider conformations within and outside the unique configuration space discussed in section 2.2.3, i.e with the dihedral angle θ in the range $0 \leq \theta \leq \pi$. As can be seen from this figure (Fig. 6), all conformations obtained from $\theta > \pi/4$ are mere orientational changes to those for which $0 \leq \theta \leq \pi/4$. The most chiral conformation of our biphenyl model is one in which the two phenyl rings are inclined at an angle of $\theta = \pi/4$, and $\chi_H = 0.1852$. In addition we calculate χ_H for 10 real biphenyl molecules which differ by a dihedral angle of 10° and obtained excellent agreement with our model, as shown in the figure. The geometry of each real molecule was optimized by minimizing the energy using a semi-empirical quantum mechanical package CaChe[25] with an augmented form of the MM3 force field.[26,27]

The χ_H that we have calculated for tetrahedra and for idealized and the minimized structures of real biphenyl molecules have been over the range $\chi_H = 0$ to 0.253 since the χ_H is based on scaling diameter of 1 for the calculation. The maximum value of χ_H is clearly less than 1 and as yet unknown. In the context $\chi_H = 0.2$ should be considered a high chirality. In order to investigate the possible range of χ_H for the simple biphenyl model molecule we considered a range of distances d_R between the two phenyl rings, with d_R = -1, 0, 0.2, 0.5, 1, and 5 as shown in Fig. 7.

Our result in this figure demonstrates that the χ_H is dependent on the model shape. For $d_R \gtrsim 0.5$ $\chi_H(\theta)$ increases linearly with θ, and as d_R increases the growth rate, at which the chirality of the model shape changes with θ, decreases and so χ_H decreases for any given θ. For $d_R \lesssim 0.5$ a crossover behaviour occurs in $\chi_H(\theta)$ at $\theta = \theta_c$ such that the growth rate becomes much lower after $\theta = \theta_c$. Thus the Hausdorff chirality χ_H of the most chiral conformation of our biphenyl model is highest for $d_R \approx 0.5$; decreases with decreasing d_R for $d_R \lesssim 0.5$ and decreases with increasing d_R for $d_R \gtrsim 0.5$.

Note that χ_H is determined by an $o - o'$ pair, i. e. for which $d(o, O')$ is highest; which in general is an $H - H'$ pair by virtue of the location of the H atoms on the extreme positions of the biphenyl molecule. The crossover behaviour in $\chi_H(\theta)$ for $d_R \lesssim 0.5$ occurs because when $d_R \lesssim 0.5$ the two phenyl rings are so close that it becomes possible to find a closer $o - o'$ pair in χ_H for $\theta \geq \theta_c$, which would not have been possible if $d_R > 0.5$. For instance, while analyzing a state of optimum superimposition, we found a situation where χ_H was determined by a $C - C'$ pair when $\theta = 32°$ ($d_R = 0$) which never occurred for $d_R > 0.5$. In the absence of this proximity factor χ_H increases linearly with θ for a given d_R.

We see that $\chi_H(\theta)$ increases with decreasing d_R for a given θ because $d(O)$ decreases with d_R. This is shown in Fig. 8 where we plot $d_{H_{\min}}(O, O')$ as a function of θ, for $d_R = -1$, 0, 1, and 5. We find that if we do not rescale $d_{H_{\min}}(O, O')$ by the diameter of the molecule, and if we do not consider the crossover, chirality is independent of d_R and increases linearly with θ.

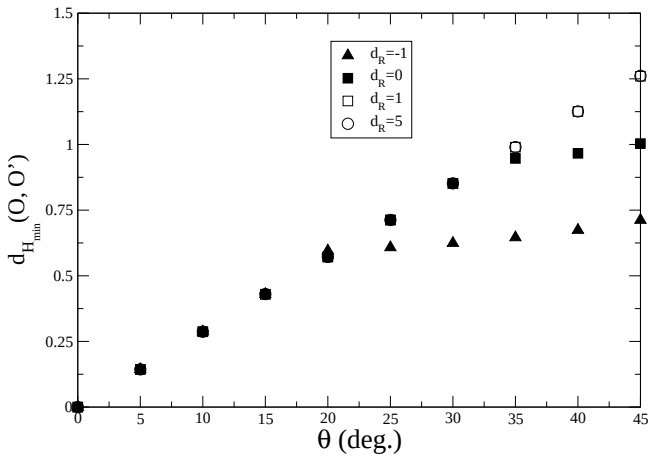

Figure 8: $d_{H_{\min}}(O, O')$ as a function of θ for $d_R = -1$, 0, 1, and 5; as discussed in the text. O is a set of the point atoms of our biphenyl model, and O' is its mirror image. Note that $d_{H_{\min}}(O, O') = d(O)\chi_H(O)$.

The above discussion could indicate a possible mechanism for chirality transfer, i. e. if we relate $\mathcal{R}_1$ and $\mathcal{R}_2(\theta > 0)$ to an achiral host system and a guest molecule, respectively; and d_R to concentration of guest molecule. If the $o - o'$ pair in a dopant and host changes to another region of the molecule a step change in chirality could occur.

3.3 Application of Hausdorff Structure Factor

The previous sections have all dealt with the problem of measuring the degree of chirality of a single molecule, and it is therefore appropriate to allow arbitrary configurations of the molecule and its mirror image, without being concerned about overlap - this physical issue is not relevant here. However, when we wish to consider the different problem of how closely physical molecules can pack, then the exclusion constraints are appropriate, and the same general procedure of simulated annealing, which has proven to be effective in solving the optimization problem posed by the Hausdorff chirality measure, is adapted to the constrained problem.

Thus the opportunity to investigate the packing of molecules in a physically realistic manner is presented when we forbid overlap through the Hausdorff structure factor $\chi_{HS}(O, Q)$. This adds the constraint that $d_{HS_{\min}}(O, Q)$, defined to be the minimum Hausdorff distance between O and Q over all positions and orientations of O and Q is greater than or equal to r_{VdW}, the Van der waals radius. We use a value of 0.184 nm as an average r_{VdW} for all molecules.

The packing of three biphenyl molecules obtained by using the algorithm of the Hausdorff structure formalism is presented in Fig. 9 as an illustration. In

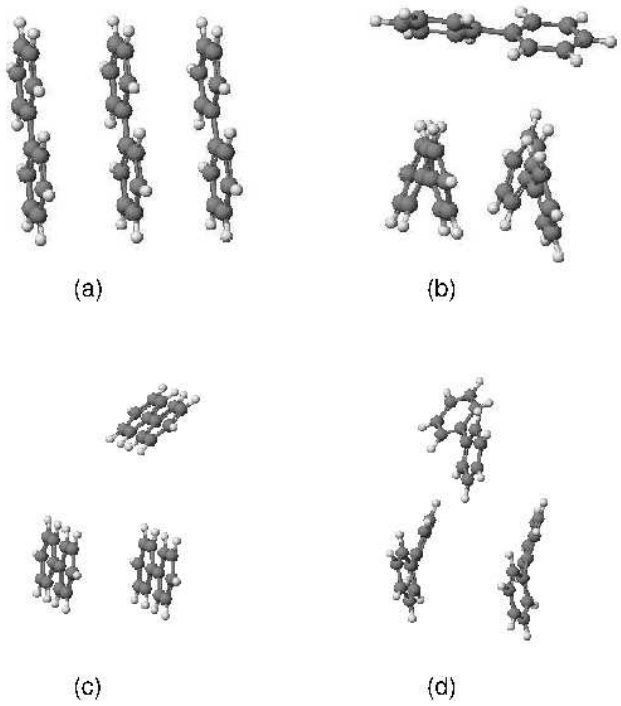

Figure 9: Three-molecule packing obtained using the Hausdorff structure algorithm. We set r_{VdW} to 1.85 in (a) and (b), and to 2.82 in (c) and (d), as described in the text. (b) and (d) are twisted conformations of the biphenyl molecule each with a dihedral angle of 34°. As seen from this figure both the twist angle and r_{VdW} affect the structure formed.

this figure, we use model 2^{33} of a biphenyl molecule in which C-H separation (δh), C-C length (d_{C-C}), and the ring-ring separation (d_R) of 0.1, 0.137, and 0.149 nm, respectively. In (a) and (c) we pack planar molecules, whereas in (b) and (d) we pack twisted molecules with a dihedral angle of 34°. We utilise the same simulated annealing algorithm with $d_{HS_{\min}}(O,Q)$ to determine χ_{HS}. First we pack two molecules, then having determined this structure we fix this and add a third. If r_{VdW} is set to 0.185 nm we find that the planar molecules pack in parallel with a separation of 0.37 nm [Fig. 9(a)]; and the twisted molecules pack with separation 0.411, 0.622, and 0.62 nm [Fig. 9(b)]. If we then increase r_{VdW} to be half minimum unit cell length of 0.564 nm[28] for a biphenyl crystal we find the packing structure changes for this fragment, with the central molecule taking up a rotated position relative to the two outside molecules that are parallel to one another. If we denote the two outside but parallel molecules (see Fig. 9) by m_1 and m_2, the third molecule by m_3, and the distance between an ith and a jth molecule by $d(m_i, m_j)$, then in this case the molecules are separated by $d(m_1, m_2) = 0.564$, $d(m_1, m_3) = 0.864$, and $d(m_2, m_3) = 0.945$ nm for Fig. 9(c); and 0.625, 0.913, 0.909 nm, respectively, for Fig. 9(d).

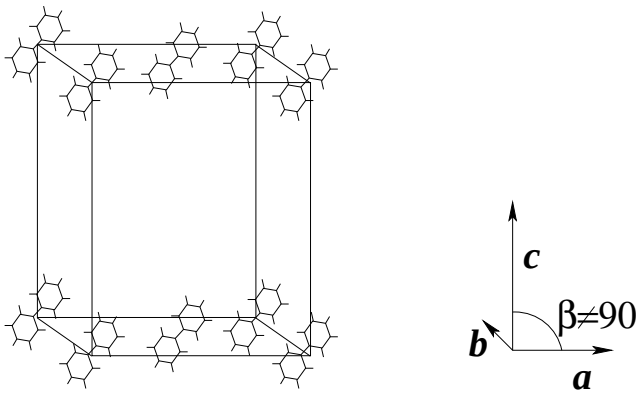

Figure 10: Crystal structure of biphenyl in phase I (not to scale) with two molecules per unit cell. Experimental data: $a = 0.812$ nm, $b = 0.564$ nm, $c = 0.947$ nm, $\beta = 95.4°$; compared to Fig. 9(c), these translates to $d(m_1, m_2) = 0.564$, $d(m_1, m_3) = 0.494$, and $d(m_2, m_3) = 0.494$ nm.

The biphenyl crystal has a monoclinic $P2_1/a(C_{2h}^5)$ phase I structure as shown in Fig. 10. It is promising that the increase in $d_{HS_{\min}}(O,Q)$ to half the minimum unit cell length shows a similar structure. Biphenyl shows a transition to incommensurate structures at higher temperatures when the twist angle between the phenyl rings is of the order of 30°-40°. Fig. 9(c) shows the structure formed by the packing of three phenyl molecules with a twist angle of 34°. Again we see that both the outside molecules are parallel to one another with the central molecule rotated. In contrast to Fig. 9(a), (b) shows that with the same $d_{HS_{\min}}(O,Q)$ of r_{VdW} of 0.185 nm but a dihedral twist the three molecules do

not pack in parallel. This demonstrates the effect of minimum separation on packing compared to the effect of the twist angle between the biphenyl rings.

4 Summary and conclusion

An application of the Hausdorff formalism for quantifying the degree of chirality of objects to the problem of the transfer of chirality between a guest molecule and its host has encouraged us to take a closer look at this method of chirality quantification as applied to real molecules. However, obtaining the minimum Hausdorff distance between two enantiomorphs is not an easy problem. In this paper we propose a new method of calculating such by using a simulated annealing algorithm.

We verified the method in three ways. First we applied it to search for the most chiral triangle and tetrahedron and obtained excellent results with those of existing solution to the problem in the literature. Secondly, we considered achiral pathways in the configuration space of tetrahedra and consistently obtained a degree of chirality $\chi_H = 0$ throughout. And thirdly, we constructed a biphenyl model, analysed its conformation space and applied the method to determine the most chiral biphenyl conformation. In this case we found that the χ_H is dependent on the molecular shape and is capable of exhibiting different scaling regions depending on the orientation of the molecule relative to its mirror image.

The results of these extensive tests confirm the validity of our method, and demonstrates its effectiveness and accuracy for possible applications as a matching algorithm in general. We have discussed a possible scenario of chirality transfer. We have proposed a Hausdorff structure factor,χ_{HS} that packs molecules by minimising $d_{HS_{\min}}(O, Q)$ with the additional constraint of no overlap within a minimum distance. We have applied this to the biphenyl molecule, utilising both the Van der Waals distance and half the minimum unit cell distance and also considered two twist angles between the phenyl rings in each case. The packing of the three molecule structures formed have been compared with real biphenyl crystal and incommensurate phases. Both the twist angle and the minimum separation affect the structure formed particularly when we utilise the Van der Waals radius. The effect is less marked when we utilise half the minimum cell length when a structure fragment (in Fig. 9) similar to that of the crystal shown in Fig. 10 is formed.

The importance of $d_{HS_{\min}}(O, Q)$ in determining packing reflected the experimental structure. Different $d_{HS_{\min}}(O, Q)$ could reflect different dopant or host concentrations. This technique presented here together with the Hausdorff chirality and structure measures offers tools to investigate the mechanisms for chirality transfer from dopants to host molecules.

Acknowledgements

The authors are very grateful to Dr Trevor Neal for the atomistic calculations. EOY thanks MMU for financial support.

References

[1] Lord Kelvin, Baltimore Lectures on Molecular Dynamics and the Wave Theory of Light, C. J. Clay and sons, London (1904)

[2] A. B. Buda and T. Auf der Heyde and K. Mislow, Angew. Chemie. Int. Ed. Engl. **31**, 989 (1992).

[3] A. B. Buda and K. Mislow, J. Am. Chem. Soc. **114**, 6006 (1992).

[4] M. Solymosi and R. J. Low and M. Grayson and M. P. Neal, J. Chem. Phys. **116**, 9875 (2002).

[5] M. Solymosi and R. J. Low and M. Grayson and M. P. Neal and M. R. Wilson and D. J. Earl, Ferroelectrics **277**, 169 (2002).

[6] M. Neal and M. Solymosi and M. R. Wilson and D. J. Earl, J. Chem. Phys. **119**, 3567 (2003).

[7] H. Kamberaj and M. A. Osipov and R. Low and M. P. Neal, Mol. Phys. **102**, 431 (2004).

[8] M. Solymosi, Molecular dynamics studies and quantification of the effect of chirality on the formation of liquid crystal mesophases, Ph. D. Thesis (2002), Coventry University, UK.

[9] H. Kamberaj, Ph. D. Thesis (2005), Manchester Metropolitan University, UK.

[10] M. A. Osipov and B. T. Pickup and D. A. Dunmur, Mol. Phys. **84**, 6, (1995); ibid. **84**, 1193 (1995).

[11] A. Ferrarini and G. J. Moro and P. L. Nordio, Liq. Cryst. **19**, 397 (1995).

[12] A. Ferrarini and P. L. Nordio, J. Chem. Soc. **2**, 455 (1998).

[13] A. Ferrarini and G. Gottarelli and P. L. Nordio and G. P. Spada", J. Chem. Phys. Soc., Perkins Trans **2**, 411 (1999).

[14] A. B. Harris and R. D. Kamien and T. C. Lubensky, Rev. Mod. Phys. **71**, 1745 (1999).

[15] A. Rassat and P. W. Fowler, Chem. Eur. J. **10**, 6575 (2004).

[16] M. P. Neal, Mol. Cryst. Liq. Cryst. (2008), in press.

[17] A. Pietropaolo and L. Muccioli and R. Berardi and C. Zannoni, Proteins: Structure, Function and Bioinformatics **70**, 667 (2008).

[18] M. P. Neal, oral presentation, SYN08, International Liquid Crystal Conference, Ljubljana, Slovenia (2004)",

[19] E. Figgemeier and K. Hiltrop, Liquid Crystals **26**, 1301 (1999).

[20] H. Stegemeyer, R. Meister, U. Hoffmann, A. Sprick, and A. Becker, J. Mater. Chem. **5**, 2183 (1995).

[21] D. Vizitiu, C. Lazar, B. J. Halden, and R. P. Lemieux, J. Am. Chem. Soc. **121**, 8229 (1999).

[22] CaChe Group, Computer-Aided Chemistry, Web: www.cachesoftware.com

[23] V. Klee suggested[2] the following formulation of Hausdorff's definition. The Hausdorff distance $h(Q, Q')$ between sets Q and Q' is the smallest number δ that has the following two properties: 1) each spherical ball of radius δ centered at any point of Q contains at least one point of Q'; 2) each spherical ball of radius δ centered at any point of Q' contains at least one point of Q.

[24] $O' = -O$ applies only to the problems involving three spatial dimensions. For the two dimensional (2-D) problem of searching for the most chiral triangle, we used a 2-D analog of our algorithm and define $G'(x_G, y_G)$ the mirror image of vertex $G(x_G, y_G)$ in $O'(E', F', G')$ as $G'(x_G, y_G) = (-x_G, y_G)$; $E' = -E$ and $F' = -F$.

[25] N. Allinger, J. Am. Chem. Soc. **111**, 8551 (1977).

[26] N. Allinger and Y. Yuh and J. Lii, J. Am. Chem. Soc. **107**, 8551 (1989).

[27] P. Pen and J. Ponder, J. Phys. Chem. B **107**, 5933 (2003).

[28] J. Trotter, Acta. Cryst. **14**, 1135 (1961).

[29] G. Casalone, C. Mariani, A. Mugnoli, and M. Simonetta, Mol. Phys. **15**, 339 (1968).

[30] G. Celebre *et. al.*, J. Chem. Soc. Far. Trans. **87**, 2623 (1991).

[31] V. Zazubovich, A. Suisalu, and J. Kikas, Phys. Rev. B **64**, 104203 (2001).

[32] P. Launois, F. Moussa, M. H. Lemee-Cailleau, and H. Cailleau, Phys. Rev. B **40**, 5042 (1989).

[33] G. B. Robertson, Nature 4788, 593 (1961).